

compounds adopt the same geometry, i.e., a capped trigonal bipyramid (see V). Thus, the rearrangement of the WO_3C_2 framework in the conversion of **1** into **2** is related formally to the rearrangement in the Os_6 framework for the overall two-electron change of $\text{H}_2\text{Os}_6(\text{CO})_{18}$ into $\text{Os}_6(\text{CO})_{18}$.

As detailed herein, evidence has been obtained for a degenerate framework rearrangement in **1**, which involves metal-metal bond cleavage in concert with hydride migration and leads to interconversion of the two possible enantiomers. This process can also be viewed as a rearrangement that interchanges the capping atom with a basal atom in the WO_3C_2 capped-square-pyramidal skeleton. The participation of a cluster framework in fluxional processes is a relatively rare phenomenon;³¹ however, certain instances have been reported recently. For example, the layered compounds $[\text{Pt}_3(\text{CO})_6]_n^{2-}$ ($n = 2-4$)³² show intramolecular rotation of the Pt_3 triangles about the stacking axis, $[\text{Rh}_9\text{P}(\text{CO})_{21}]^{2-}$ ³³ apparently undergoes a $C_{4v} \leftrightarrow D_{3h}$ polyhedral rearrangement, and $\text{H}_2\text{FeRuOs}_2(\text{CO})_{13}$ ³⁴ exhibits metal atom framework movement coupled with hydrogen migration.

An especially interesting aspect of **2** is the presence of a terminal hydride ligand associated with the tungsten atom. This ligand was located directly from the crystallographic analysis for molecule B. Although there have been several metal carbonyl cluster compounds with terminal hydride ligands in the literature,^{17,18,35} only in one other case, $(\text{H})(\mu-$

$\text{H})\text{Os}_3(\text{CO})_{10}(\text{PPh}_3)_{18}$,¹⁸ was a terminal hydride ligand successfully located directly by X-ray methods. The ^1H NMR chemical shifts of terminal hydride ligands are generally found at lower field than those of corresponding bridging hydride ligands,³⁶ but the exceptionally low-field position (*downfield* of SiMe_4) of the hydride signal for **2** is unique for a cluster compound. Several mononuclear tungsten(VI) hydride compounds display signals in this low-field region.³⁷ Given the electronegativity difference between tungsten and osmium, it is not unreasonable to assign the pair of electrons in a normal W-Os σ bond totally to the osmium atom, as for a W-C or W-H σ bond. In this way the tungsten atom in **2** is viewed as bonded to six anionic ligands (C_5H_5^- , H^- , 2C^- , 2Os^-) and a neutral donor osmium center ($\text{Os}(1)$), i.e., its formal oxidation state is VI. Although this analysis is clearly just a formalism, its message is consistent with the structural evidence for **2**, i.e., that the tungsten center is significantly more electron poor than the osmium centers are.

Acknowledgment. This research was supported by the National Science Foundation through Grants CHE81-00140 (J.R.S., University of Illinois) and CHE80-23448 (M.R.C., SUNY—Buffalo). We thank Dr. C. H. McAteer for valuable discussions regarding NMR work. Mass spectra were obtained at the University of Illinois in part under a grant from the National Institute of General Medical Sciences (Grant GM 27029). Acknowledgment is also made for the use of NMR instrumentation in the Regional Instrumentation Facility at the University of Illinois (NSF Grant CHE 79-16100).

Supplementary Material Available: Tables of calculated hydrogen atom positions for **1** (Table II-B), anisotropic thermal parameters for **1** and **2** (Tables III and V), and observed and calculated structure factors for **1** and **2** (50 pages). Ordering information is given on any current masthead page.

- (30) Mason, R.; Thomas, K. M.; Mingos, D. M. P. *J. Am. Chem. Soc.* **1973**, *95*, 3802.
 (31) Band, E.; Muetterties, E. L. *Chem. Rev.* **1978**, *78*, 639.
 (32) Brown, C.; Heaton, B. T.; Towl, A. D. C.; Chini, P.; Fumagalli, A.; Longoni, G. *J. Organomet. Chem.* **1979**, *181*, 233.
 (33) Gladfelter, W. L.; Geoffroy, G. L. *Inorg. Chem.* **1980**, *19*, 2579.
 (34) Vidal, J. L.; Walker, W. E.; Pruett, R. L.; Shoening, R. C. *Inorg. Chem.* **1979**, *18*, 129.
 (35) (a) $[\text{H}_4\text{Re}_4(\text{CO})_{15}]^{2-}$: Ciani, G.; Albano, V. G.; Immirz, A. *J. Organomet. Chem.* **1976**, *121*, 237. (b) $\text{HO}_3\text{Re}(\text{CO})_{15}$: Churchill, M. R.; Hollander, F. J. *Inorg. Chem.* **1977**, *16*, 2493. (c) $[\text{H}_2\text{Ir}_4(\text{CO})_{10}]^{2-}$: Ciani, G.; Manassero, M.; Albano, V. G.; Canziani, F.; Giordano, G.; Martinengo, S.; Chini, P. *J. Organomet. Chem.* **1978**, *150*, C17. (d) $\text{HO}_3(\text{CO})_{10}(\text{PEt}_3)(\text{CF}_3\text{CCHCF}_3)$: Dawoodi, Z.; Mays, M. J.; Raithby, P. R. *J. Chem. Soc., Chem. Commun.* **1979**, 721. (e) $\text{H}_2\text{Os}_3(\text{CO})_{10}(\text{CN-}t\text{-Bu})$: Adams, R. D.; Golembki, N. M. *Inorg. Chem.* **1979**, *18*, 1909.

- (36) (a) Kaesz, H. D.; Saillant, R. B. *Chem. Rev.* **1972**, *72*, 231. (b) Jesson, J. P. In "Transition Metal Hydrides"; Muetterties, E. L., Ed.; Marcel Dekker: New York, 1971; pp 75-201.
 (37) For instance, the hydride signal for $\text{W}(\text{CH})(\text{PMe}_3)_3\text{Cl}_2\text{H}$ occurs at δ 4.53 but that for $\text{W}(\text{CMe}_2)(\text{dmpe})_2\text{H}$ at δ -6.27: Holmes, S. J.; Clark, D. N.; Turner, H. W.; Schrock, R. R. *J. Am. Chem. Soc.* **1982**, *104*, 6322.

Contribution from the Institut für Anorganische Chemie, Universität Hannover, 3000 Hannover 1, FRG

Structural Investigations on Solid Tetraphosphorus Hexaoxide

M. JANSEN* and M. MOEBES

Received April 23, 1984

Single crystals of P_4O_6 have been grown from the melt. By X-ray diffraction at $-5 \pm 1^\circ\text{C}$ the space group ($P2_1/m$), the unit cell ($a = 642.2$ (1) pm, $b = 787.7$ (2) pm, $c = 678.6$ (3) pm, $\beta = 106.1$ (1)°, $V = 329.8 \times 10^6$ pm³, $d_{\text{calcd}} = 2.215$ g cm⁻³, $Z = 2$, $M_r = 219.89$), and the crystal and molecular structure have been determined. As compared to those in gaseous P_4O_6 , the bonding angles remain almost unchanged, while—obviously because of crystal forces—the molecule as a whole is expanded; $\bar{d}(\text{P}-\text{O}) = 165.3$ pm (solid) and 163.8 pm (gas). With respect to the globular shape of P_4O_6 , the molecular packing is unexpected: rods extending along [100] are formed by aligning P_4O_6 molecules with protrusions of one unit fitting into the hollows of the next. Between the liquid and solid states, no plastically crystalline phase was detected. At $-45 \pm 4^\circ\text{C}$ a structural phase transition of probably higher order to a triclinic low-temperature modification occurs.

Introduction

The phosphorus oxides P_4O_{6+n} ($n = 0-4$) and their derivatives seem ideally suited for comparative studies on chemical bonding within the cage molecules¹ as well as on the packing

of the similarly shaped units in the crystalline state.² These studies have been hampered by incomplete or insufficient reliable structural information. The problems with crystal structure determinations on this type of compound arise from a strong tendency to disorder^{1a} or from formation of solid solutions ($\text{P}_4\text{O}_{7.9} = 0.1\text{P}_4\text{O}_7 + 0.9\text{P}_4\text{O}_8$). Recently the

- (1) (a) Cotton, F. A.; Riess, J. G.; Stults, B. R. *Inorg. Chem.* **1983**, *22*, 133.
 (b) Casabianca, F.; Pinkerton, A. A.; Riess, J. G. *Inorg. Chem.* **1977**, *16*, 864.

- (2) Jansen, M.; Moebs, M. Z. *Kristallogr.* **1982**, *159*, 283.

preparation of pure and crystalline P_4O_7 from P_4O_6 and O_2 in one step was achieved.⁴ The crystal structure of P_4O_7 was the key to the detection of close packing relationships among P_4O_7 , P_4O_8 , P_4O_9 , and P_4O_{10} , thus giving an explanation for the readily formed solid solutions among them.² In this context, the crystal structure of the terminating link of the series, P_4O_6 , is of particular interest. We have, therefore, performed structural investigations on solid P_4O_6 within the temperature range -100 to $+20$ °C.

Experimental Section

P_4O_6 was purified by distillation ($+40 \rightarrow -10$ °C), leaving an unidentified reddish residue. Because of its extreme sensitivity to moisture and oxygen, all X-ray experiments were performed on samples in small capillaries, filled and sealed under dry argon.

Crystal Growth. Single crystals of P_4O_6 (mp 23 °C) were grown in situ on a Syntex P₂ diffractometer. For this purpose a capillary of 0.3-mm diameter, filled with the liquid sample to a height of approximately 20 mm, was attached to the diffractometer, which was equipped with a low-temperature device. The top of the capillary protruded through a small hole at the center of a heated ($+30$ °C) metal screen into a cold nitrogen gas stream (-20 °C). Crystal growth was achieved by slowly moving the screen, thus introducing the whole capillary into the gas stream.⁵

This procedure was repeated until a single crystal had formed, which, according to oscillation photographs, seemed suitable for X-ray diffraction experiments.

Data Collection. Intensity data were collected at -5 ± 1 °C on a Syntex P₂ automated diffractometer using graphite-monochromated Mo K α radiation ($\lambda = 0.71069$ Å). The orientation of the crystal and preliminary lattice constants were determined from 25 carefully centered reflections in the range $10^\circ < \theta < 20^\circ$. Systematic absences ($0k0$, $k \neq 2n$) and monoclinic symmetry indicated $P2_1$ and $P2_1/m$ as possible space groups. In the course of the structure determination, the latter proved to be the correct one. The principal crystallographic data are as follows: $a = 642.2$ (1) pm; $b = 787.7$ (2) pm; $c = 678.6$ (3) pm; $\beta = 106.1$ (1)° (obtained from Guinier powder data, $T = -10$ °C); $V = 329.8 \times 10^6$ pm³; $d_{\text{calc}} = 2.215$ g cm⁻³; $Z = 2$; $\mu_{\text{Mo K}\alpha} = 9.9$ cm⁻¹; $M_r = 219.89$. A total of 1361 reflections, $\pm h, k, l$, with $1^\circ < 2\theta < 65^\circ$ were collected in the ω -scan mode. Scan rates and width were $1-29.3^\circ$ min⁻¹ and 2° , respectively. The intensities of three standard reflections, monitored after every 100 reflections, showed no significant change during data collection.

Solution and Refinement of the Structure. The structure was determined by direct phasing of 227 reflections with $E > 1.2$, the solution with the "best" figures of merit generating an E map that contained the approximate positional coordinates of all atoms. The refinement (based on 1277 independent reflections) of a scale factor, all positional parameters, and finally anisotropic temperature factors gave the discrepancy indices $R_1 = \sum ||F_o| - |F_c|| / \sum |F_o| = 0.086$ and $R_2 = \sum w^{1/2} ||F_o| - |F_c|| / \sum w^{1/2} |F_o| = 0.096$, the parameters of the weighting scheme $w = k / (\sigma^2(F_o) + gF_o^2)$ being refined to $k = 3.942$ and $g = 0.0007$. The parameter shifts in the last cycle were less than 0.01 times the estimated standard deviation.

All calculations were performed on a CYBER 76 using the program system SHELX-76.⁶ The atomic scattering factors of phosphorus and oxygen were taken from ref 7. The final difference map ranged between 0.89 and -0.71 e/Å³. The variances were devoid of systematic variation with $(\sin \theta) / \lambda$ and F / F_{max} .

When compared to the present standard in structure determination with diffractometer data, the R values seem somewhat high. Nevertheless, we consider at least the structural geometric results reliable, as the more sensitive anisotropic temperature parameters are physically meaningful (cf. next section) and the difference map is without prominent features.

Table I. Positional and Thermal Parameters^a for P_4O_6

atom	x	y	z	$U_{\text{eq}}^b, \text{Å}^2$
P1	7412 (2)	2500	4891 (2)	559 (9)
P2	3524 (2)	2500	6413 (2)	588 (9)
P3	7432 (2)	4372 (2)	8649 (2)	681 (8)
O1	4760 (5)	2500	4605 (5)	577 (23)
O2	4791 (4)	4104 (4)	7801 (4)	641 (18)
O3	8082 (4)	4104 (4)	6499 (4)	613 (18)
O4	8089 (6)	2500	9719 (5)	730 (22)

^a Multiplied by 10^4 ; standard deviations in parentheses. ^b $U_{\text{eq}} = \frac{1}{3} \sum_i \sum_j U_{ij} a_i^* a_j^* a_i a_j$.

Table II. Intramolecular Distances (pm) and Angles (deg) and the Shortest Intermolecular Contacts (pm) (Esd's in Parentheses)

P1-O1 [O3]	166.2 (4) [164.9 (3)]	166.8 (4) ^a [165.6 (3)] ^a	
P2-O1 [O2]	163.5 (4) [165.1 (3)]	164.0 (4) ^a [165.8 (3)] ^a	
P3-O2 [O3; O4]	164.6 (3) [163.8 (3); 164.8 (2)]	165.2 (3) ^a [164.2 (3); 165.4 (2)] ^a	
O1-P1-O3	98.6 (1)	P1-O3-P3	127.0 (2)
O3-P1-O3	100.2 (1)	P2-O2-P3	126.4 (2)
O1-P2-O2	99.4 (2)	P3-O4-P3	127.3 (3)
O2-P2-O2	100.1 (1)	O1-O2 ^b	318.5
O2-P3-O3 [O4]	99.7 (1) [98.8 (2)]	P2-O3 ^b	331.2
O3-P3-O4	100.4 (2)	P3-P3 ^b	394.4
P1-O1-P2	127.4 (2)		

$P_4O_6(s)$	P-O	165.3 ^{a,c}	$P_4O_6(g)$	P-O	163.8
	P-O-P	127.0 ^c		P-O-P	126.7
	O-P-O	99.5 ^c		O-P-O	99.8

^a Corrected for rigid-body motion. ^b Intermolecular distances. ^c Mean values.

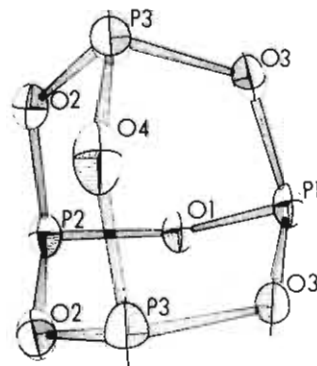


Figure 1. View of the molecule including atomic numbering (ellipsoids at the 20% probability level).

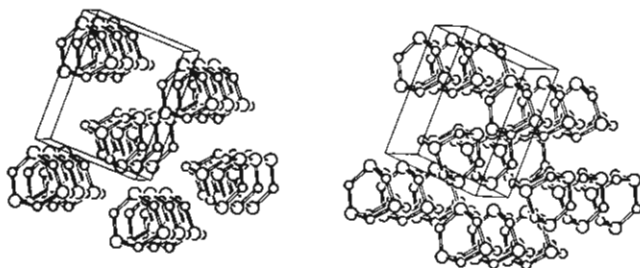


Figure 2. ORTEP stereoview of the unit cell showing the molecular packing.

Powder Diffraction: Low-Temperature Investigation. A sample of liquid P_4O_6 , sealed in a Lindemann capillary (o.d. = 0.3 mm), was cooled rapidly to -150 °C, thus crystallizing within less than 1 s, and Guinier powder diagrams were recorded. Comparison of the calculated and observed intensity profiles revealed strong discrepancies caused by the preferred orientation of the crystallites. This is supported by the observation that repeated melting and rapid crystallization yielded powder diagrams with the reflections at constant scattering angles but varying intensities. Low-temperature Guinier photographs indicate

(3) Jost, K.-H. *Acta Crystallogr.* **1966**, *21*, 34.

(4) Moebs, M.; Jansen, M. *Z. Anorg. Allg. Chem.* **1984**, *514*, 39. Jansen, M.; Voss, M. *Angew. Chem.* **1981**, *93*, 120.

(5) Simon, A.; Deiseroth, H.-J.; Westerbeck, E.; Hillenkötter, B. *Z. Anorg. Allg. Chem.* **1976**, *423*, 203.

(6) Sheldrick, G. M. SHELX System of Programs, University of Cambridge, England, 1976 (unpublished).

(7) "International Tables for X-ray Crystallography"; Kynoch Press: Birmingham, England, 1974; Vol. IV.

Table III. Comparison of Bond Lengths (pm) in Phosphorus Oxides^a

	P ₄ O ₆	P ₄ O ₇	P ₄ O ₈	P ₄ O ₉	P ₄ O ₁₀
P ^{III} -O _a	165.3 (3)	164.4 (4)	163.3 (10)		
P ^{III} -O _b		168.4 (5)	166.8 (13)	166.1 (13)	
P ^V -O _b		159.5 (4)	157.6 (14)	160.5 (16)	
P ^V -O _c			159.6 (9)	159.0 (12)	157.5 (4)
P ^V -O _d		145.0 (5)	141.4 (13)	141.8 (14)	141.0 (2)
					151.0 (4)
ref	this work	4, 13	3, 9	14, 15	12

^a O_a, O_b, and O_c are bridging oxygens between P^{III}/P^{III}, P^{III}/P^V, and P^V/P^V, respectively; O_d is in a terminal position.

a structural phase transition at -45 ± 4 °C.

Results

Table I reports the positional parameters, and Figures 1 and 2 illustrate the molecular structure with the atomic numbering scheme and a stereoview of the molecular packing, respectively. In Table II the intramolecular distances and angles as well as the shortest intermolecular contacts are given and the average values, which are computed under the assumption of T_d symmetry, are compared to the respective distances and angles of gaseous P₄O₆.

Tables of observed and calculated structure factors, thermal vibration parameters (experimental and calculated according to the model of rigid-body motion), and d spacings as derived from Guinier photographs are available as supplementary material.

Discussion

The crystal structure consists of P₄O₆ molecular units with site symmetry m , the mirror plane passing through P1, P2, O1, and O4 (cf. Figure 1). Geometrical analysis ("best planes" and angles between their normals) of the molecular structure reveals the point group to be T_d within the limits of experimental error, which is the same as for the isolated molecule. The anisotropic thermal parameters are quantitatively interpretable in terms of rigid-body motion of the molecule.⁸ The center giving a symmetric S tensor (0.61, 0.25, 0.61) differs only slightly from the barycenter of the molecule (0.64, 0.25, 0.71). The bond distances, both uncorrected and corrected for the effect of rigid-body motion, are significantly larger than those determined by electron diffraction on gaseous P₄O₆.⁹ Intermolecular interactions, which seem to be of the van der Waals type as indicated by the shortest intermolecular contacts $d(\text{O}-\text{O}) = 319$ pm (van der Waals radius¹⁰ of O 152 pm), obviously account for this fact. Considering all available information on P-O distances in phosphorus oxides (Table III), a general tendency—not very pronounced, indeed—is apparent: in the series P₄O₆, P₄O₇, and P₄O₈ the P^{III}-O-P^{III} P-O bond length decreases from 165 through 164 to 163 pm; P^V-O-(terminal) shortens from P₄O₇ (145 pm) to P₄O₉ (141 pm). In general this can be attributed to increasing nuclear charges resulting from increasing oxygen content within the molecule, which should effect a contraction of the whole unit. The above mentioned structural feature may be explained in more detail in terms of increasing effective charge on the phosphorus(III) atoms with increasing number of phosphorus(V) atoms [and decreasing effective charge on pentavalent P with increasing amounts of phosphorus(III)]. The latter interpretation is supported by ³¹P NMR chemical shifts as determined for the species P₄O₆Y_n (Y = O, S, Se; $n = 1-4$).¹¹

In order to obtain insight into bonding properties of *closo* phosphorus compounds, Cotton et al. performed extensive and systematic work on P₄(NMe)₆X_n (X = O, S; $n = 0-4$).¹ Because of considerable variations in bond lengths—even in those that should be equal, presuming idealized symmetry—the conclusion was drawn that as a common feature these compounds exhibit a high degree of disorder in crystal packing and the molecules are inherently deformable, thus lowering the precision in structural data as determined by X-ray methods. Moreover, this statement was generalized and extended to the phosphorus oxides. However, from our point of view such a general extension is not permissible. The supposition that e.g. P₄O₁₀ behaves like a "deflated tennis ball" does not hold, if one retains in mind that the P₄O₁₀ units consist of corner-sharing tetrahedral PO₄ groups, which are known to behave rather rigidly. In the *closo*-phosphorus methylimides, however, the—at least latent—tendency of nitrogen to adopt a pyramidal surrounding and to undergo inversion introduces configurational instabilities.

The librational motion in phosphorus oxides is pronounced but can be successfully treated by the procedure of Schomaker and Trueblood,⁸ as is shown by the results on P₄O₆ and P₄O₇. From our experience a very crucial point is the purity of the investigated samples, for related molecules are readily accommodated by formation of mixed crystals. Especially from our results on P₄O₇, we feel encouraged to reinvestigate P₄O₈, P₄O₉, and P₄O₁₀, for which the presently available structural information is indeed not very convincing.

The manner of molecular packing in solid P₄O₆ is rather unexpected: rods are formed by aligning P₄O₆ units along their threefold axes with protrusions (phosphorus and its lone pair) on one unit fitting into hollows (center of P₃O₃ rings) in the next unit. The approximately close-packed rods extend parallel to the a axis of the monoclinic system; cf. Figure 2. Usually, globular molecules adopt highly space-filling sphere packings that derive from the crystal structures of metals, as may be demonstrated by the examples As₄O₆ (fcc arrangement), P₄ (α -manganese), and P₄O₁₀ (bcc). By careful inspection it was ensured that P₄O₆ adopts none of these packings. Another interesting feature is that, in spite of the almost spherical molecular shape, low melting point, and high vapor pressure, P₄O₆ does not form a plastically crystalline phase. This presents a marked and presently inexplicable contrast to P₄, which has a higher melting point (44 °C) and exists over a broad temperature range as a plastic-crystalline phase.

Because of the restricted intensity data obtained on the low-temperature phase of P₄O₆ by powder methods, only qualitative conclusions about its crystal structure can be drawn. When the transition temperature is passed, the powder diagram shows no discontinuity, thus classifying the phase transition as probably being of higher order. The symmetry changes from monoclinic to triclinic. Probably only slight changes in the packing of the molecules are responsible for the phase transition.

Acknowledgment. The authors gratefully acknowledge the Deutsche Forschungsgemeinschaft and the Fonds der Chemie for support of this work.

Registry No. P₄O₆, 12440-00-5.

Supplementary Material Available: Listings of observed and calculated structure factors, anisotropic thermal parameters, and observed d values (10 pages). Ordering information is given on any current masthead page.

- (8) Schomaker, V.; Trueblood, K. N. *Acta Crystallogr., Sect. B* **1968**, *B24*, 63.
 (9) Beagley, B.; Cruickshank, D. W. J.; Hewitt, T. G.; Jost, K. H. *Trans. Faraday Soc.* **1969**, *65*, 1219.
 (10) Bondi, A. *J. Phys. Chem.* **1964**, *68*, 441.

- (11) Walker, M.; Peckenpaugh, D. E.; Mills, J. *Inorg. Chem.* **1979**, *18*, 2792.
 (12) Cruickshank, T. G. *Acta Crystallogr.* **1964**, *17*, 677.
 (13) Jost, K. H.; Schneider, M. *Acta Crystallogr., Sect. B* **1981**, *B37*, 222.
 (14) Jost, K. H. *Acta Crystallogr.* **1964**, *17*, 1593.
 (15) Beagley, B.; Cruickshank, D. W. J.; Hewitt, T. G.; Haaland, A. *Trans. Faraday Soc.* **1967**, *63*, 836.